

## Dynamic tuning of an infrared hybrid-metamaterial resonance using vanadium dioxide

T. Driscoll,<sup>1,a)</sup> S. Palit,<sup>2</sup> M. M. Qazilbash,<sup>1</sup> M. Brehm,<sup>3</sup> F. Keilmann,<sup>3</sup> Byung-Gyu Chae,<sup>4</sup> Sun-Jin Yun,<sup>4</sup> Hyun-Tak Kim,<sup>4</sup> S. Y. Cho,<sup>2</sup> N. Marie Jokerst,<sup>2</sup> D. R. Smith,<sup>1,2</sup> and D. N. Basov<sup>1</sup>

<sup>1</sup>Physics Department, University of California-San Diego, La Jolla, California 92093, USA

<sup>2</sup>Electrical and Computer Engineering Department, Duke University, P.O. Box 90291, Durham, North Carolina 27708, USA

<sup>3</sup>Abt. Molekulare Strukturbiologie, Max-Planck-Institut für Biochemie and Center for NanoScience, 82152 Martinsried, München, Germany

<sup>4</sup>IT Convergence & Components Lab, ETRI, Daejeon 305-350, Republic of Korea

(Received 8 April 2008; accepted 2 June 2008; published online 14 July 2008)

We demonstrate a metamaterial device whose far-infrared resonance frequency can be dynamically tuned. Dynamic tuning should alleviate many bandwidth-related roadblocks to metamaterial application by granting a wide matrix of selectable electromagnetic properties. This tuning effect is achieved via a hybrid-metamaterial architecture; intertwining split ring resonator metamaterial elements with vanadium dioxide ( $\text{VO}_2$ )-a material whose optical properties can be strongly and quickly changed via external stimulus. This hybrid structure concept opens a fresh dimension in both exploring and exploiting the intriguing electromagnetic behavior of metamaterials. © 2008 American Institute of Physics. [DOI: 10.1063/1.2956675]

Advances in the recently emerging field of metamaterials include the development and demonstration of devices for subwavelength imaging,<sup>1</sup> cloaking,<sup>2</sup> ultrafast optoelectric switching,<sup>3</sup> and more. So far, these devices have most often relied on geometrically fixed electromagnetic resonances which restrict operation to a single frequency<sup>4,5</sup> or narrow band.<sup>6</sup> Real-time tuning of the resonant response is one possible way to overcome limitations of bandwidth. Demonstrations of tuning have been made for microwave frequencies using integrated rf electrical components.<sup>7</sup> At infrared and higher frequencies, such components are unavailable, and other means of implementing tuning must be found.<sup>8</sup> Our hybrid split ring resonator vanadium dioxide (SRR- $\text{VO}_2$ ) device accomplishes this, granting a resonance tuning range of 20% or more.

Our device is made of 100 nm thick gold SRRs lithographically fabricated on a 90 nm layer of  $\text{VO}_2$  [see Fig. 1(b)]. The  $\text{VO}_2$  is grown on a sapphire substrate, and thoroughly characterized by electrical<sup>9</sup> and optical measurements.<sup>10</sup>  $\text{VO}_2$  undergoes a thermally triggered insulator-to-metal phase transition<sup>11</sup> that corresponds to a four orders of magnitude change in conductivity. The SRR is the most common and best characterized implementation of electromagnetic metamaterials.<sup>12–14</sup> It responds resonantly to in-plane electric fields, and out-of-plane magnetic fields. The way which the  $\text{VO}_2$  and SRR layers interact is what makes this hybrid-metamaterial interesting. The thickness of the lithographic gold comprising the SRRs and of the  $\text{VO}_2$  film are both much less than the in-plane periodicity of the SRR array (20  $\mu\text{m}$ ). Metamaterial arrays like this have been shown to form *effective* material layers whose electromagnetic thickness is approximately the period of the array,<sup>14,15</sup> rather than the physical thickness of the lithographic gold. In this arrangement, the local electromagnetic fields of the SRR

overlap the  $\text{VO}_2$  layer [see Fig. 1(c)] and intertwine with the  $\text{VO}_2$  material response. The  $\text{VO}_2$  film thus becomes part of this effective material layer—due to its proximity to the SRRs and thin size compared to the array periodicity. Together they form a hybrid metamaterial—blending the properties of the  $\text{VO}_2$  film with those of the discrete SRR array.

The resonance frequency of the SRR metamaterial is highly sensitive to the dielectric property of any material placed nearby, especially in the vicinity of the SRR gaps.<sup>16</sup> This circumstance, along with the following distinctive dielectric property of  $\text{VO}_2$ , enables the realization of a dynamically tunable SRR- $\text{VO}_2$  hybrid metamaterial. Near its insulator-to-metal phase transition,  $\text{VO}_2$  exhibits a divergent *bulk* permittivity [see Fig. 2(c)]. This modifies the local fields of the SRR within and around the gap region, acting like a tunable dielectric inside a capacitor. The resonance frequency of the SRR- $\text{VO}_2$  hybrid system is expected to decrease as  $\text{VO}_2$  permittivity increases: a behavior anticipated from a simplified *RLC*-circuit model of SRR response. Ex-

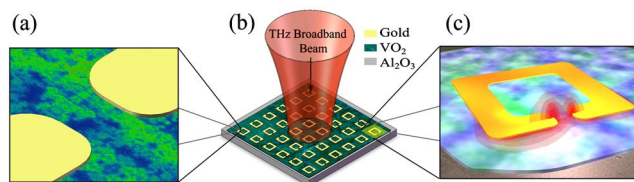


FIG. 1. (Color online) Sketch of the vanadium dioxide SRR hybrid-metamaterial. (a) Close-up of the SRR gap, sketched on top of a near-field image of a  $\text{VO}_2$  film during phase transition. This comparison illustrates that the  $\text{VO}_2$  percolating metallic grains (green) which emerge from the insulating host (blue) are much smaller than SRR gap. The sSNIM data is taken at 342 K. (b) Device layout and experimental setup. Gold SRRs of period 20  $\mu\text{m}$  are lithographically fabricated above a 90 nm thick  $\text{VO}_2$  layer, which has been grown on sapphire. The resonance of this hybrid-metamaterial device is probed in transmission. (c) Blow-up of a single SRR with electric field total amplitude results from a numerical solver, illustrating the overlap of the SRR fields with the  $\text{VO}_2$  film.

<sup>a)</sup>Electronic mail: tdriscol@physics.ucsd.edu.

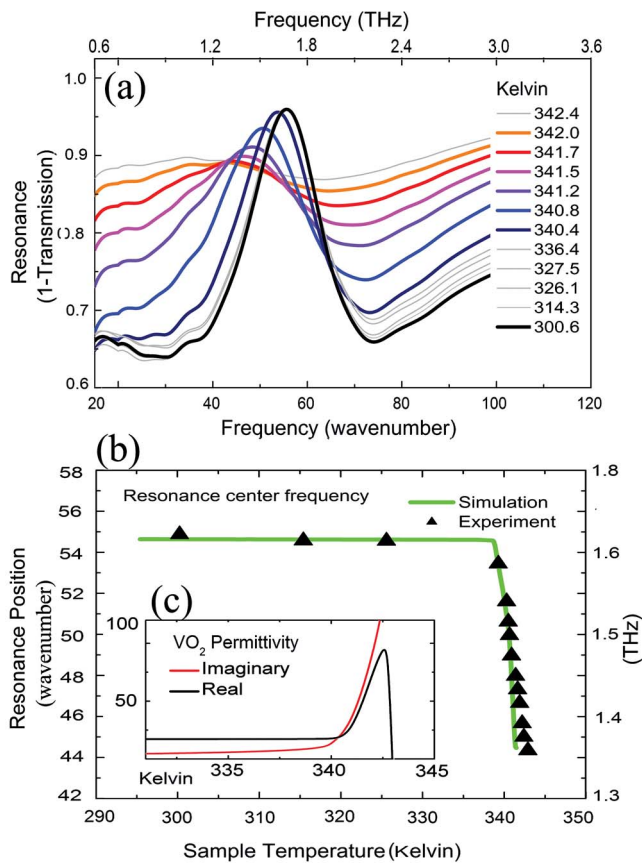


FIG. 2. (Color online) Dynamic tuning of the SRR  $w_0$ -resonance. (a) Transmission spectra through the hybrid metamaterial device at increasing sample temperatures. The resonance frequency decreases by nearly 20% as the vanadium dioxide passes through its metal insulator transition. (b) Resonance frequency as a function of temperature. (c) (inset in b)  $\text{VO}_2$  Bruggeman effective-medium permittivity.

perimental results as well as numerical simulations, reported below, substantiate these expectations.

The observed divergent permittivity of the bulk  $\text{VO}_2$  is understood to be due to the percolative nature of the phase transition. During its phase transition,  $\text{VO}_2$  exhibits the emergence and growth of tiny (5–10 nm) metallic puddles [see Fig. 1(a)] in the insulating host. Figure 1(a) illustrates this, showing near-field composition data obtained via scattering scanning near-field infrared microscope (sSNIM), overlaid on a sketch of the 3  $\mu\text{m}$  wide SRR gap. The *effective medium* response of the bulk  $\text{VO}_2$  material comprised of these metal and insulating puddles is described by the Bruggeman model.<sup>10</sup> This arrangement is interesting as it utilizes one nanometer-scale effective-medium (formed by metallic puddles in the  $\text{VO}_2$  insulation host) within another micron-size effective medium (formed by the periodic SRR array).

To probe this hybrid metamaterial, we perform Fourier transform infrared transmission spectroscopy of our device. We focus normally incident linearly polarized light from a mercury lamp onto a 3  $\text{mm}^2$  spot on the 1  $\text{cm}^2$  sample. The SRR array is oriented such as to electrically excite the SRR by taking advantage of the asymmetrical in-plane dipole moment created in the long and short legs of the SRR.<sup>17,18</sup>

In Fig. 2, we display transmission spectra for our hybrid device. The room temperature spectra reveal a strong resonance with a peak at 55  $\text{cm}^{-1}$  [see Fig. 2(a)]. As we increase the temperature of the device,  $\text{VO}_2$  begins its transition and

the observed resonance peak frequency decreases. The tuning of the resonance through the  $\text{VO}_2$  transition can be mapped by plotting the peak frequency versus temperature [see Fig. 2(b)]. The resultant curve shows a sharp onset of tuning as the phase transition begins, and has a tuning range of 20%. At temperatures above 342 K, the resonance becomes heavily damped due to the increasing conductivity of the  $\text{VO}_2$  layer. Eventually, the interconnecting  $\text{VO}_2$  metallic puddles electrically short the SRR entirely, giving us the ability to turn the resonance off at temperatures above 343 K.

We substantiate our experimental observations numerically—simulating the metamaterial using the finite-integration time-domain code package Microwave Studio by CST, Inc. All three constituents of the device (SRR,  $\text{VO}_2$ ,  $\text{Al}_2\text{O}_3$  substrate) are included. These numerical results agree very well with our experimental data—showing a room temperature resonance at 55  $\text{cm}^{-1}$ . Simulations for elevated temperatures [green tuning curve shown in Fig. 2(b)] use Bruggeman permittivity values for  $\text{VO}_2$  taken from Fig. 2(c),<sup>10</sup> and also agree well with experimental data. The accuracy of Microwave Studio for the prediction of the resonance tuning of our SRR- $\text{VO}_2$  hybrid is important, since metamaterial design advances are largely reliant on such numerical simulators.

In order to evaluate the parameter space where this hybrid-metamaterial device enables tunable electromagnetic properties, we retrieve permittivity and permeability values for the metamaterial layer. This is done by modeling the transmission through a two-layer device (hybrid SRR+ $\text{VO}_2$  and  $\text{Al}_2\text{O}_3$  substrate) using the Fresnel equations. Electromagnetic oscillators are assigned to the material of each layer, and then fit to the observed spectra.<sup>14</sup> Literature values for the permittivity of  $\text{Al}_2\text{O}_3$  are used for the substrate.<sup>19</sup> The oscillator used for the hybrid metamaterial layer is a modified Lorentzian—incorporating effects arising from the spatial dispersion present in the SRR array.<sup>20</sup> This recent advance in our fitting procedure gives a noticeable improvement in fit over previous oscillator models.<sup>21</sup> Figure 3 shows the retrieved real permittivity and permeability. The room temperature permittivity exhibits an expected strong resonance. Room temperature permeability also shows a weak antiresonance, even in our electric excitation configuration. This is an artifact of the SRR array periodicity; spatial dispersion acts to couple the permittivity resonance to a permeability antiresonance. This effect has been routinely observed for metamaterials with periodicity such as ours—in the range of one-tenth of a wavelength.<sup>22</sup>

At temperatures above 340 K, the retrieved permittivity and permeability resonances both redshift. This frequency shift follows the transition from insulator to metal with temperature in  $\text{VO}_2$ . Losses in the  $\text{VO}_2$  metallic puddles also damp the resonance, decreasing the amplitude. Any non-tunable metamaterial allows only a *single* pair of permittivity and permeability curves. In contrast, the shaded area in Fig. 3 illustrates a range of permittivity and permeability values accessible with the help of our hybrid SRR- $\text{VO}_2$  device. Through careful control of the sample temperature, we can select any permittivity-permeability curve pair in the shaded region. Electromagnetic flexibility of this kind is immensely valuable in device design and operation.

The accuracy of our oscillator-fitting model in replicating the observed experimental spectra highlights the essence

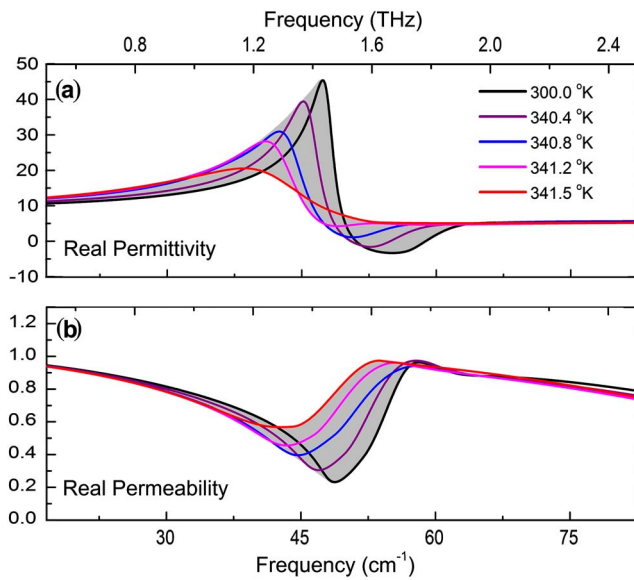


FIG. 3. (Color online) Experimentally retrieved permittivity and permeability bandwidth for the hybrid metamaterial. (a) Permittivity values for the SRR-VO<sub>2</sub> hybrid layer in our device. (b) Permeability values. The shaded area illustrates the complete range of values accessible with the help of our hybrid SRR-VO<sub>2</sub> device

of the hybrid-metamaterial approach. Physically, our gold SRR array and VO<sub>2</sub> film comprise two distinct layers, each only  $\sim 100$  nm thick. Electromagnetically, however, these two layers are exceedingly well represented by one single hybrid-material layer with combined properties of SRR and VO<sub>2</sub>. As mentioned, the electromagnetic thickness of a SRR array is approximated by the array periodicity, which can be quite large compared to the physical thickness of the SRR. It is this large electromagnetic thickness which allows us to easily combine the properties of other nearby materials with those of the metamaterial, forming a hybrid-metamaterial.

We stress that the phase transition in VO<sub>2</sub> may be triggered optically<sup>23</sup> or electrically<sup>24</sup> as well as thermally, thus enabling photonic or electric control of the resonance in this hybrid metamaterial. In these cases, one can envision locally triggered sections of VO<sub>2</sub> for pixel-like tuning of the metamaterial. Taking advantage of advanced device architectures can also expand the range of tuning, by making every attempt to maximize the SRR electric flux inside the VO<sub>2</sub>. Simulations performed employing embedded SRRs in thicker 500 nm VO<sub>2</sub> reveal a resonance shift of up to 40%—twice the range of our demonstrated device. Our demonstra-

tion of dynamic tuning in this SRR-VO<sub>2</sub> configuration suggests the potential for rich physics and interesting effects in other hybrid-metamaterial devices employing magnetic, nonlinear, or other materials. Combining the wide ranging phenomena found in natural materials with the electromagnetic design control offered by metamaterials may act to expand the usefulness of each.

The authors are grateful for and wish to acknowledge funding for this project from AFOSR MURI (W911NF-04-1-0247), FA 9550-06-01-0279, and ETRI.

- <sup>1</sup>J. B. Pendry, *Phys. Rev. Lett.* **85**, 18 (2000).
- <sup>2</sup>J. B. Pendry, D. Schurig, and D. R. Smith, *Science* **312**, 1780 (2006).
- <sup>3</sup>H.-T. Chen, W. J. Padilla, J. M. O. Zide, A. C. Gossard, A. J. Taylor, and R. D. Averitt, *Nature (London)* **444**, 597 (2006).
- <sup>4</sup>D. Schurig, J. J. Mock, B. J. Justice, S. A. Cummer, J. B. Pendry, A. F. Starr, and D. R. Smith, *Science* **314**, 977 (2006).
- <sup>5</sup>Z. Liu, H. Lee, Y. Xiong, C. Sun, and X. Zhang, *Science* **315**, 1686 (2007).
- <sup>6</sup>T. Driscoll, D. N. Basov, A. F. Starr, P. M. Rye, S. Nemat-Nasser, D. Schurig, and D. R. Smith, *Appl. Phys. Lett.* **88**, 081101 (2006).
- <sup>7</sup>I. V. Shadrivov, S. K. Morrison, and Y. S. Kivshar, *Opt. Express* **14**, 9344 (2006).
- <sup>8</sup>H.-T. Chen, J. F. O'Hara, A. K. Azadi, A. J. Taylor, R. D. Averitt, D. B. Shrekenhamer, and W. J. Padilla, *Nat. Photonics* **2**, p. 295 (2008).
- <sup>9</sup>Y. J. Chang, J. S. Yang, D. H. Kim, T. W. Noh, D. W. Kim, E. O. Kahng, B. Kahng, and J. S. Chung, *Phys. Rev. B* **76**, 075118 (2007).
- <sup>10</sup>M. M. Qazilbash, M. Brehm, B.-G. Chae, P.-C. Ho, G. O. Andreev, B.-J. Kim, S. J. Yun, A. V. Balatsky, M. B. Maple, F. Keilmann, H.-T. Kim, and D. N. Basov, *Science* **318**, 1750 (2007).
- <sup>11</sup>A. Zylbersztejn and N. F. Mott, *Phys. Rev. B* **11**, 4383 (1975).
- <sup>12</sup>W. J. Padilla, D. N. Basov, and D. R. Smith, *Mater. Today* **9**, 28 (2006).
- <sup>13</sup>D. R. Smith and J. B. Pendry, *J. Biomed. Opt.* **23**, 3 392 (2006).
- <sup>14</sup>T. Driscoll, D. N. Basov, W. J. Padilla, J. J. Mock, and D. R. Smith, *Phys. Rev. B* **75**, 115114 (2007).
- <sup>15</sup>D. R. Smith, D. Schurig, and J. J. Mock, *Phys. Rev. E* **74**, 036604 (2006).
- <sup>16</sup>T. Driscoll, G. O. Andreev, D. N. Basov, S. Palit, S. Y. Cho, N. M. Jokerst, and D. R. Smith, *Appl. Phys. Lett.* **91**, 062511 (2007).
- <sup>17</sup>W. J. Padilla, A. J. Taylor, C. Highstrete, M. Lee, and R. D. Averitt, *Phys. Rev. Lett.* **96**, 107401 (2006).
- <sup>18</sup>N. Katsarakis, G. Konstantinidis, A. Kostopoulos, R. S. Penciu, T. F. Gundogdu, M. Kafesaki, E. N. Economou Th. Koschny, and C. M. Soukoulis, *Opt. Lett.* **30**, 1348 (2005).
- <sup>19</sup>D. Billard, F. Gervais, and B. Piriou, *Int. J. Infrared Millim. Waves* **1**, 4 (1980).
- <sup>20</sup>R. Liu, T. J. Cui, D. Huang, and B. Zhao, *Phys. Rev. E* **76**, 026606 (2007).
- <sup>21</sup>T. Driscoll, G. O. Andreev, D. N. Basov, S. Palit, T. Ren, J. Mock, S.-Y. Cho, N. M. Jokerst, and D. R. Smith, *Appl. Phys. Lett.* **90**, 092508 (2007).
- <sup>22</sup>T. Koschny, P. Markos, and D. R. Smith, *Phys. Rev. E* **68**, 065602 (2003).
- <sup>23</sup>M. Rini, A. Cavalleri, R. W. Schoenlein, R. Lopez, L. C. Feldman, R. F. Haglund, L. A. Boatner, and T. E. Haynes, *Opt. Lett.* **30**, 1 (2004).
- <sup>24</sup>H. T. Kim, B. G. Chae, D. H. Youn, S. L. Maeng, G. Kim, K. Y. Kang, and Y. S. Lim, *New J. Phys.* **6**, 52 (2004).